

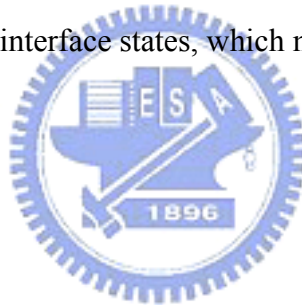
Appendix A

Effects of Nitrogen Dose on the Negative Bias Temperature Instability of pMOSFETs with Thin Gate Oxide

A.1 Background and Motivation

Threshold voltage drift due to device degradation, especially in deep submicron regime, is a major reliability concern in analog and mixed-signal circuit applications. Negative Bias Temperature Instability (NBTI) of p⁺-gated MOSFETs with thin gate dielectrics has been reported as one of the most serious reliability issues due to its large threshold voltage shift [24-25]. The NBTI degradation could become the limiting lifetime factors for p-channel devices when the gate oxide thickness is scaled to 3.5 nm and less. Despite many research efforts, detailed NBTI degradation mechanism is still not well understood. This is further complicated by the fact that the reliability of p⁺-gated MOSFETs is affected by several other factors, such as hot carrier effects [A1] and boron penetration [A2]. Recently, nitrogen incorporation has often been applied to prevent boron penetration, channel hot carrier effects, and improve surface roughness at the interface. However, several reports have also indicated that the nitrogen at the interface could aggravate NBTI degradation due to

the smaller activation energy E_a associated with NBTI stressing [A3-A5]. In this study, the nitrogen dose effects implanted at different regions, i.e., surface channel or source/drain extension, were investigated. Moreover, to simulate switching operation of an inverter in a real circuit, the gate voltage of the test device is deliberately switched between negative and positive biases with a cycle time of 2000 seconds during NBTI testing (namely, Dynamic NBTI, DNBTI) [A6]. In addition, two stressing field conditions (i.e., $V_G=1$ V and $E_{OX}=-13$ MV/cm, both at 125 °C) were executed to compare the DNBTI effects. Charge pumping current was also measured to investigate the evolution of interface states, which may recover after stressing.



A.2 Device Fabrication

P-channel MOSFETs were fabricated on 6-in p-type wafers with resistivity of 15-20 Ω -cm. P^{31} implant with an energy of 120 keV and a dose of 7.5×10^{13} cm^{-2} was performed for n-well formation. Local oxidation of silicon (LOCOS) was used for device isolation. As^+ implant with an energy of 100 keV and a dose of 1×10^{13} cm^{-2} was performed for threshold voltage (V_{TH}) adjustment, followed by various nitrogen implants (i.e., 5×10^{13} , 1×10^{14} , and 5×10^{14} cm^{-2} ; all at 10 keV). After stripping the sacrificial oxide, a final 2.8 nm gate oxide was grown in N_2O ambient. For comparison, control samples were grown in O_2 ambient, either without or with

nitrogen implantation (10 keV, $5 \times 10^{13} \text{ cm}^{-2}$). Next, all wafers were combined to receive a 200 nm poly-Si gate deposition. The poly-Si gate layer was then patterned and etched to define transistor gate length, varying from $10 \mu\text{m}$ to $0.8 \mu\text{m}$, all with a channel width of $100 \mu\text{m}$. Shallow S/D extensions were next formed by BF_2 implant (10 keV, $4 \times 10^{14} \text{ cm}^{-2}$). Nitrogen ions (i.e., 10 keV, with dose at 5×10^{13} or $5 \times 10^{14} \text{ cm}^{-2}$) were implanted into the S/D extension regions at this stage to compare the effects of different nitrogen incorporating regions on the reliability of pMOSFETs. After the formation of TEOS sidewall spacer (200nm), deep p^+ - source/drain junctions were formed by BF_2 implantation. Afterwards, wafers were annealed by rapid thermal annealing (RTA) at $1020 \text{ }^\circ\text{C}$ for 20 sec. A 550 nm TEOS oxide layer was then deposited and etched to form contact holes. Next, a Ti/TiN/Al-Si-Cu/TiN 4-layer metal was deposited and patterned to complete contact metallization. Finally, $400 \text{ }^\circ\text{C}$ forming gas sintering was performed before electrical characterizations using an HP4156 system. NBTI stressing tests were performed using a temperature-regulated hot chuck at temperatures ranging from $25 \text{ }^\circ\text{C}$ to $125 \text{ }^\circ\text{C}$.

A.3 Experimental Results and Discussion

Figure A.1 shows the schematic for NBTI stress setup. Both substrate and well electrodes are grounded. Fig. A.2(a) shows the stress time dependence of threshold

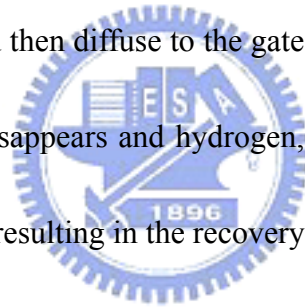
voltage degradation for various pMOSFETs with different nitrogen implant doses (i.e., N₂O oxide, 10 keV, with dose of 5×10^{13} , 10^{14} , 5×10^{14} cm⁻², respectively, and O₂ oxide w/o N₂ implantation) in the channel. Devices were stressed at E_{OX}=-13 MV/cm and T = 125 °C with other terminals (i.e., source, drain, well, and substrate) grounded. ΔV_{TH} is defined as $V_{TH}(t) - V_{TH}(0)$ for transistors with L/W=0.8 $\mu\text{m}/100 \mu\text{m}$. It is noted that higher nitrogen implantation in the channel results in higher threshold voltage degradation. This is consistent with previous reports [A3-A5], in which lower activation energy E_a due to nitrogen was found in the interface. This increases interface states density N_{it} and aggravates threshold voltage degradation for devices with higher nitrogen dose. It should be noted that the control device using O₂ oxide and without any nitrogen implant depicts the best NBTI resistance among all splits. Compared to its counterpart with N₂O oxynitride and 5×10^{14} cm⁻² nitrogen implantation, the control device with pure oxide exhibits a smaller threshold voltage shift by as much as 20 mV after 10000-sec stressing. Fig. A.2(b) shows comparisons for N₂O-oxide devices with different nitrogen implant doses (i.e., 5×10^{13} and 5×10^{14} cm⁻², both at 10 keV) at the S/D extension region. It is interesting to note that higher nitrogen implantation at the S/D extension region also aggravates the NBTI degradation. This can be explained by the locally enhanced degradation reactions between holes and oxide near the S/D, and the nitrogen may diffuse to the interface

during RTA processing step [A7] or lateral scattering of ion implantation.

Figs. A.3(a) and (b) show the stress time dependence of V_{TH} degradation under high electrical stressing field (i.e., $E_{OX}=-15$ MV/cm) and low temperature conditions (i.e., $T = 25$ °C), with all other terminals (i.e., source, drain, well, and substrate) grounded. It can be seen that the NBTI degradation under low temperature and high electrical field increases as nitrogen dose increases, similar to that shown in Fig. 5.2 for stressing under high temperature (i.e., $T = 25$ °C) and low electrical field (i.e., $E_{OX}=-13$ MV/cm). Fig. A.4(a) shows the recombined charge per cycle Q_{ss} [A8] as a function of frequency for various pMOSFETs with different nitrogen doses (N_2O oxide, 10keV, with nitrogen dose of 5×10^{13} , 10^{14} , 5×10^{14} cm⁻², respectively; and O_2 oxide w/o N_2 implantation.) in the channel. The recombined charge per cycle Q_{ss} is deduced from I_{cp}/f , where I_{cp} is the maximum charge pumping current and f is the frequency. The slope of Q_{ss} versus $\log(f)$ is proportional to the interface state density D_{it} [A8]. It can be clearly seen that the O_2 oxide control device without N_2 implant depicts the steepest slope, indicating the worst D_{it} behavior due to boron penetration [A9]. While devices that received nitrogen implantation show almost the same magnitude of D_{it} , irrespective of the implant dose. This can be explained by the suppression of boron penetration by nitrogen implant. Fig. A.4(b) shows the results for N_2O oxide devices that received different nitrogen doses (i.e., 5×10^{13} and 5×10^{14}

cm^{-2} , both at 10 keV) at S/D extension. It can be seen that these devices depict smaller slope than those shown in Fig. A.4(a). We believe this is because the nitrogen implantation in the poly-Si gate during S/D extension implant effectively suppresses the boron penetration [A10]. However, larger nitrogen dose at S/D extension may cause local defects and enhance NBTI degradation, as shown in Fig. A.2(b). Fig. A.5 shows the threshold voltage degradation under high-temp low-field NBTI stressing conditions (i.e., 125 °C, -13 MV/cm) with different well biases (i.e., $V_{\text{well}}=0, 1, 2$ V) for all splits. Well bias increases the energy band bending of silicon well as the S/D and substrate terminals are grounded. So the injected substrate hot holes increase the interface states [A3]. The schematic figure has been reported in Ref [A3]. At $V_{\text{well}}=1$ V, the threshold voltage degradation is only slightly larger than those at $V_{\text{well}}=0$ V even after 10^4 seconds stressing, indicating only marginal substrate hot hole generation. However, at $V_{\text{well}}=2$ V, threshold voltage degradation is significantly enhanced (i.e., by more than 25 mV, compared to those at $V_{\text{well}}=0$ V), suggesting that the substrate hot holes dominate the threshold voltage degradation at $V_{\text{well}}=2$ V. It is also worth noting here that the splits with higher nitrogen implant in either the channel or S/D extension region are more sensitive to the generation of substrate hot holes. Figures A.6(a) and (b) show the dynamic NBTI effects (DNBTI), which simulate the inverter operation of CMOS circuit. The period of each cycle is 2000


seconds. Figs. A.6(a) and (b) show the stress time dependence of threshold voltage degradation for N₂O oxide pMOSFETs with different nitrogen doses (i.e., 5×10^{13} , 10^{14} , and 5×10^{14} cm⁻²) in the channel and S/D extension, respectively. The DNBTI stress conditions were $T = 125$ °C, and $E_{OX} = -13$ MV/cm during negative gate stressing, and $V_G = 1$ V during positive gate stressing. Other terminals (source, drain, well, and substrate) were grounded. It is worth noting that the recovery after second negative state is smaller than that after first positive state. Under high temperature and negative bias stressing, holes from the inversion layer could break the Si-H bond and increase interface trap N_{it} , and then diffuse to the gate electrode [A11]. Under positive bias, the channel inversion disappears and hydrogen, broken by holes, then migrates back to the Si/SiO₂ interface, resulting in the recovery of Si dangling bonds. We found that the degradation during negative bias period is proportional to the nitrogen implant dose implanted either in the channel or S/D extension due to the resultant lower activation energy E_a . Figs. A.7(a) and (b) show the stress time dependence of maximum charge pumping current measured during DNBTI stressing (100°C, $E_{OX} = -13$ MV/cm) for N₂O oxide pMOSFETs with different nitrogen doses (5×10^{13} , 10^{14} , and 5×10^{14} cm⁻²) implanted in either the channel or S/D region. The results for the O₂ oxide device without N₂ implant are also shown for comparison. Triangle pulse and 1M Hz frequency was employed for charge pumping current measurement.



Although the interface state density D_{it} of pure oxide is the highest, as previously shown in Fig. A.4(a), due to its poor boron penetration retardation, $\Delta I_{cp_{max}}$ for the pure oxide split is smaller than those for N_2O splits. In particular, the split of N_2O oxide with $5 \times 10^{14} \text{ cm}^{-2}$ nitrogen dose depicts the worst $\Delta I_{cp_{max}}$ degradation, which is consistent with the observed NBTI effects shown in Fig. A.2(a). Furthermore, at positive state stressing, i.e., during the period of 2000-4000 seconds, $\Delta I_{cp_{max}}$ only decreases slightly. This implies that interface states recovers during positive state stressing. Fig. A.7(b) also shows that higher nitrogen implantation at S/D extension causes larger $\Delta I_{cp_{max}}$. Fig. A.8 compares the DNBTI effects for O_2 control and N_2O oxide device with $1 \times 10^{14} \text{ cm}^{-2}$ nitrogen dose. During the state of NBTI, the magnitude of ΔV_{TH} of N_2O device is worse than that of O_2 control due to the lower activation energy of nitrogen. However, after positive state recovery, ΔV_{TH} of both splits was comparable. This indicates that the broken Si bonds could be passivated effectively after positive state stressing, and the degree of recovery is larger for the N_2O device. This may be due to the lower activation energy E_a of nitrogen, which could enhance the recovery magnitude. Figs. A.9(a) and (b) show the dynamic NBTI effects for devices with different nitrogen doses. The condition of negative state was set at 125 °C, $E_{OX} = -13 \text{ MV/cm}$, while that of positive state was $E_{OX} = 13 \text{ MV/cm}$ (V_G was positive and equal to that of NBTI stressing). Other terminals (source, drain, well, and

substrate) were grounded under both conditions. It is very interesting to note that only 10 seconds passivation is depicted for all splits, afterwards the threshold voltage degradation increases continuously. Compared to the 1 V positive stressing, recovery strength increases as the positive bias increases. The enhanced threshold voltage degradation may be due to the TDDB effects. Higher electrical field across the gate dielectric could damage the gate dielectric and aggravate threshold voltage degradation.

A.4 Summary



NBTI effects with different nitrogen implant doses and regions were investigated. Higher nitrogen dose, either in the channel or in the S/D extension region, could aggravate threshold voltage degradation due to the lower activation energy. We found that substrate hot hole injection also aggravates NBTI effects, especially for $V_{\text{well}} = 2\text{V}$. In addition, higher nitrogen implant dose also enhances substrate hot holes. The reduction of maximum charge pumping current $I_{\text{cp}_{\text{max}}}$ after positive gate bias stressing indicates interface state recovery, suggesting that the passivation of the threshold voltage is due to interface state recovery. Finally, the interface state recovery of oxynitride is more significant than that of O_2 oxide due to the lower activation energy.

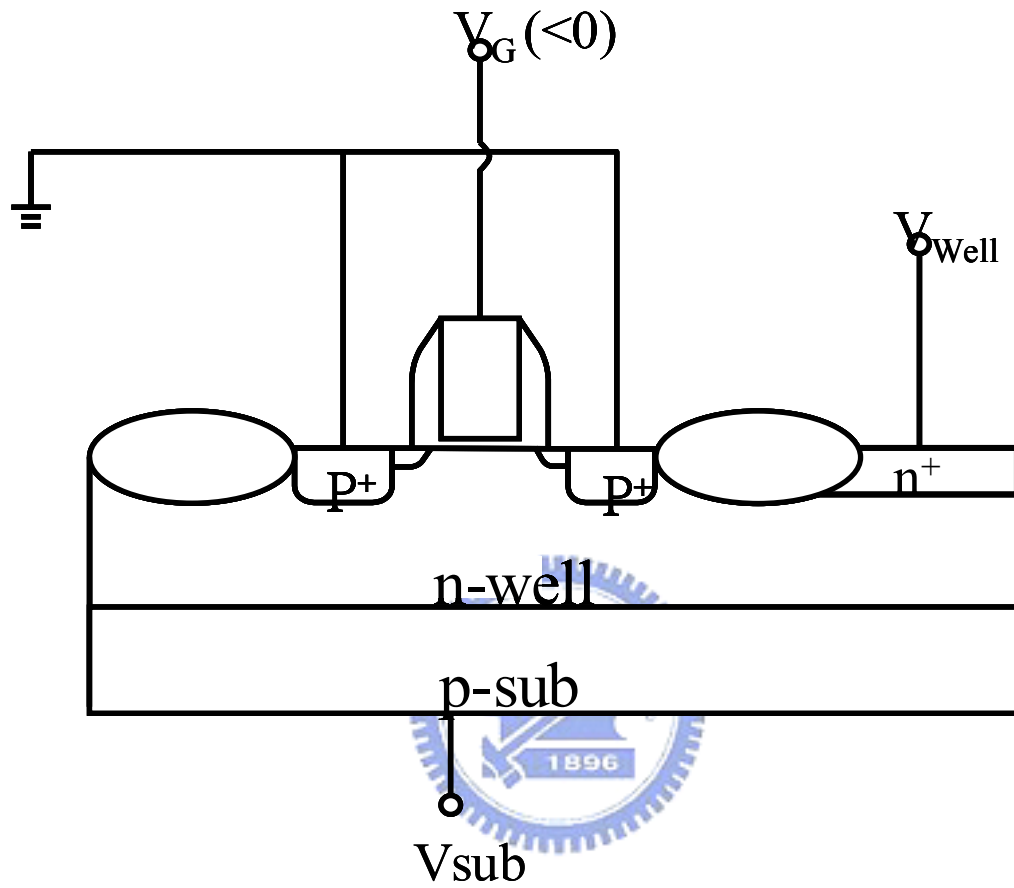
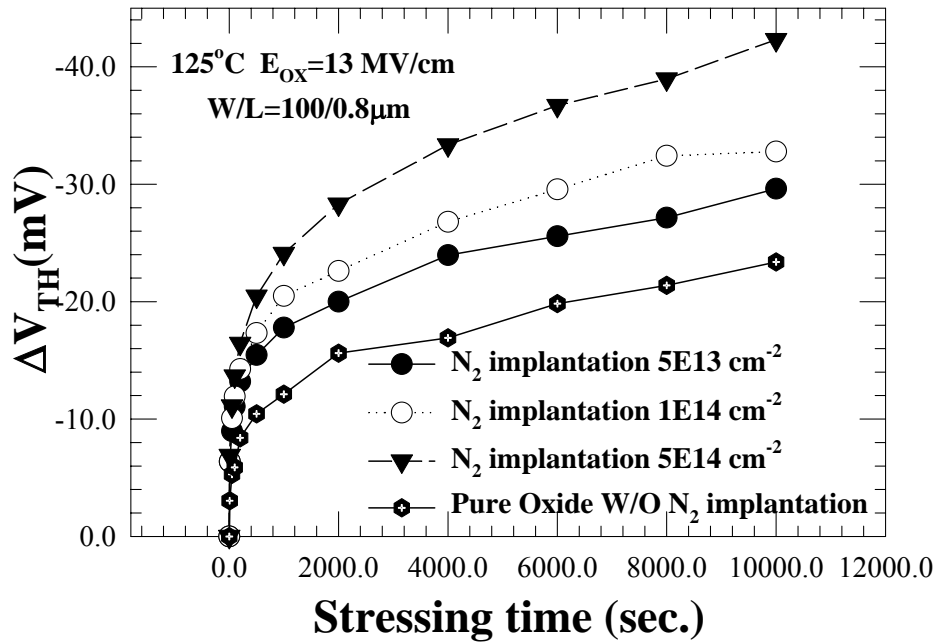
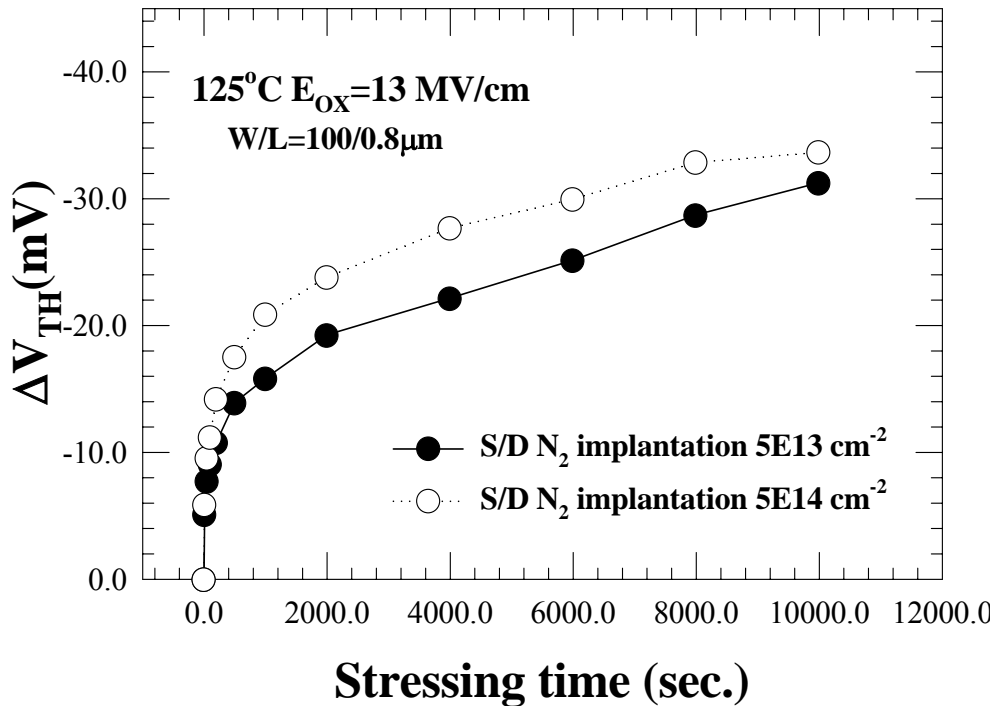


Fig. A.1 Schematics for NBTI stress setup. Both substrate and well electrodes are grounded.

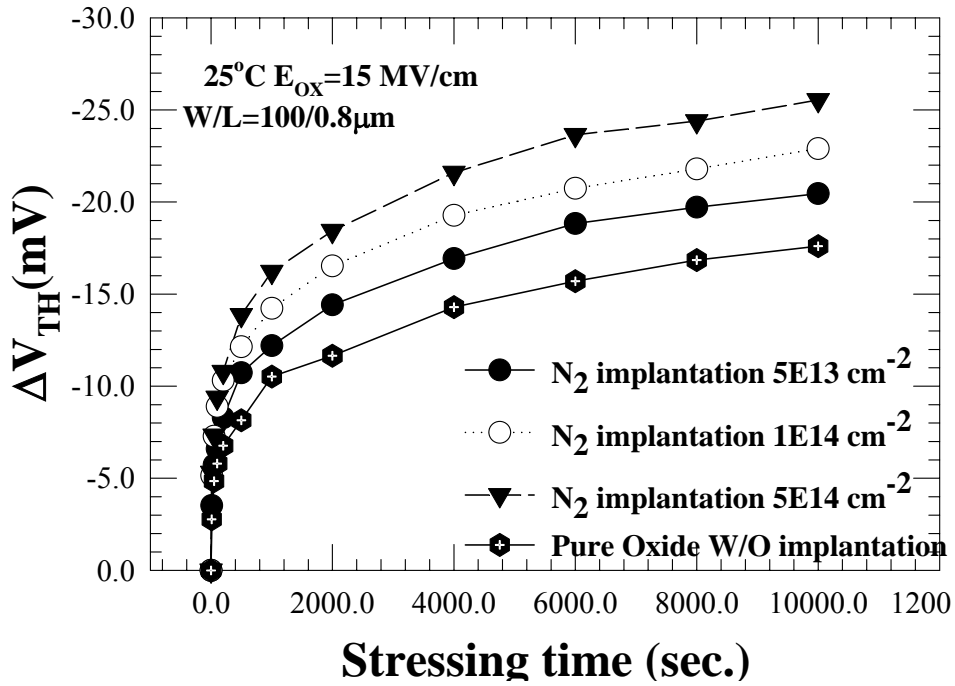


(a)

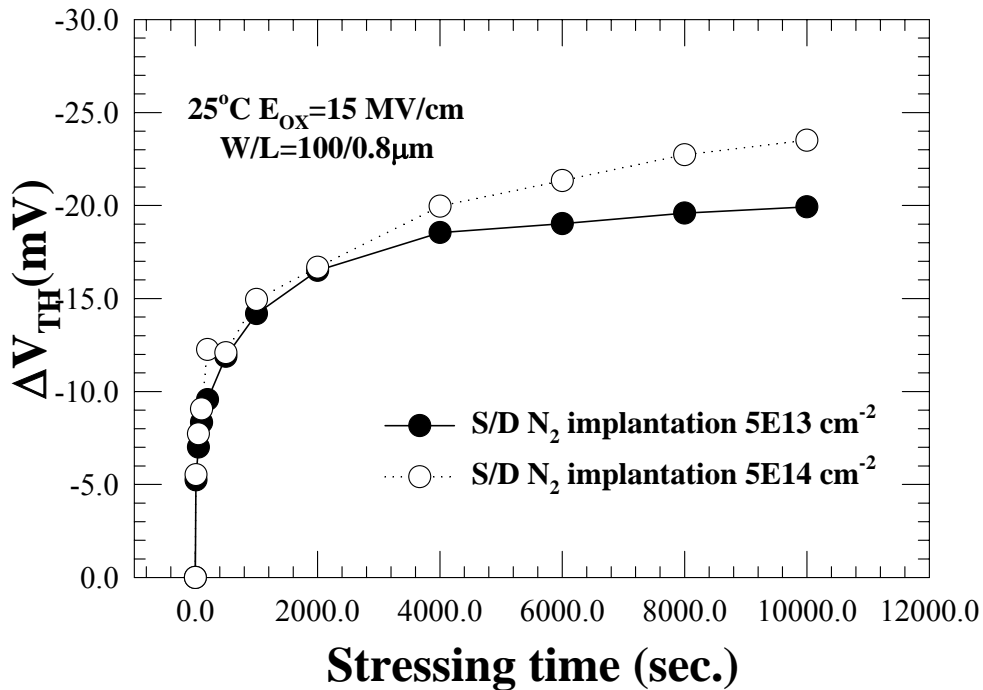


(b)

Fig. A.2 Stress time dependence of threshold voltage degradation for various pMOSFETs that received different nitrogen implant doses in (a) the channel and (b) the S/D extension. The stressing condition is 125 °C, $E_{OX}=13$ MV/cm. (N_2O oxide: 10keV, 5×10^{13} , 10^{14} , 5×10^{14} cm $^{-2}$, and O_2 oxide: w/o implantation.)

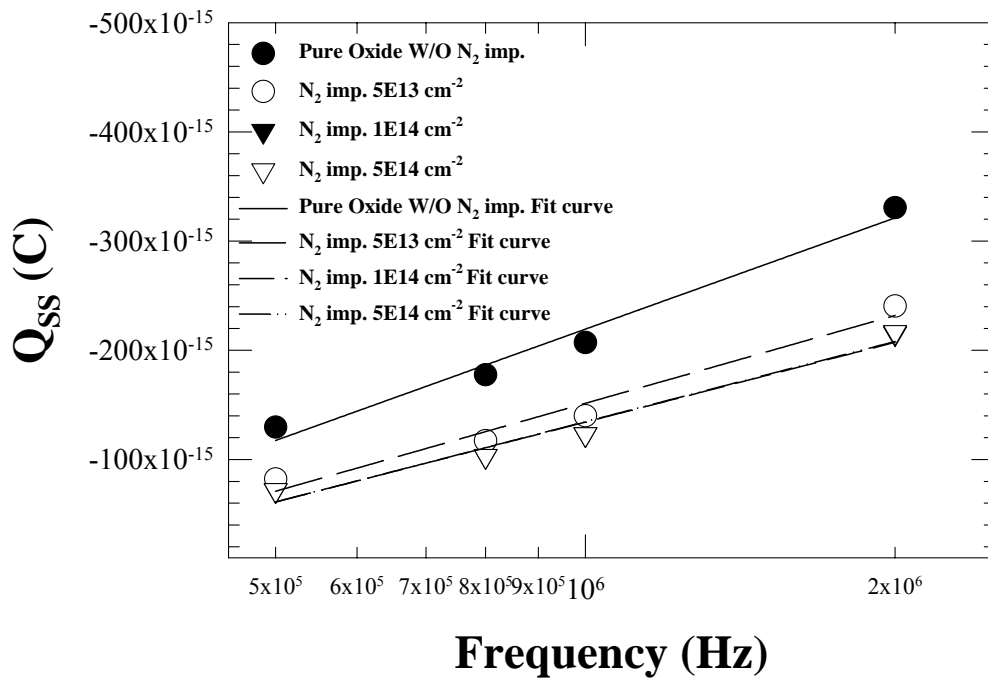


(a)

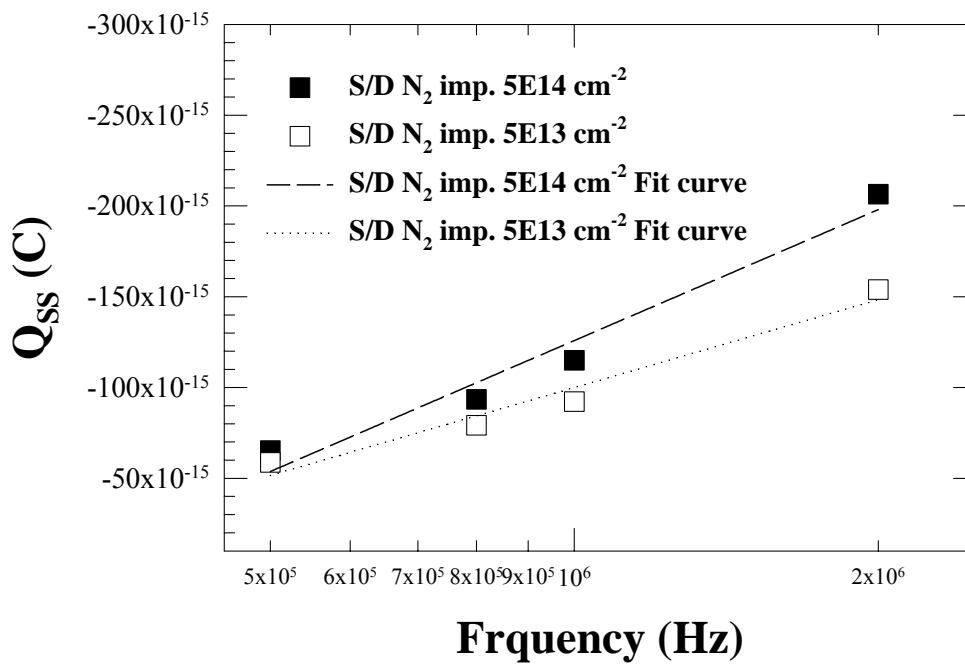


(b)

Fig. A.3 (a) Stress time dependence of threshold voltage degradation for pMOSFETs with different nitrogen implant doses implantation in (a) the channel and (b) the S/D extension. The stressing condition is 25 °C, $E_{ox}=15$ MV/cm. (N_2O oxide: 10 keV, 5×10^{13} , 10^{14} , 5×10^{14} cm^{-2} , and O_2 oxide: w/o implantation.)



(a)



(b)

Fig. A.4 (a) Q_{ss} (charge pumping current I_{cp} / frequency f) versus frequency for pMOSFETs with different nitrogen implant doses in (a) the channel and (b) the S/D extension region. (N_2O oxide, 10keV , 5×10^{13} , 10^{14} , $5 \times 10^{14} \text{ cm}^{-2}$, and O_2 oxide w/o implantation.)

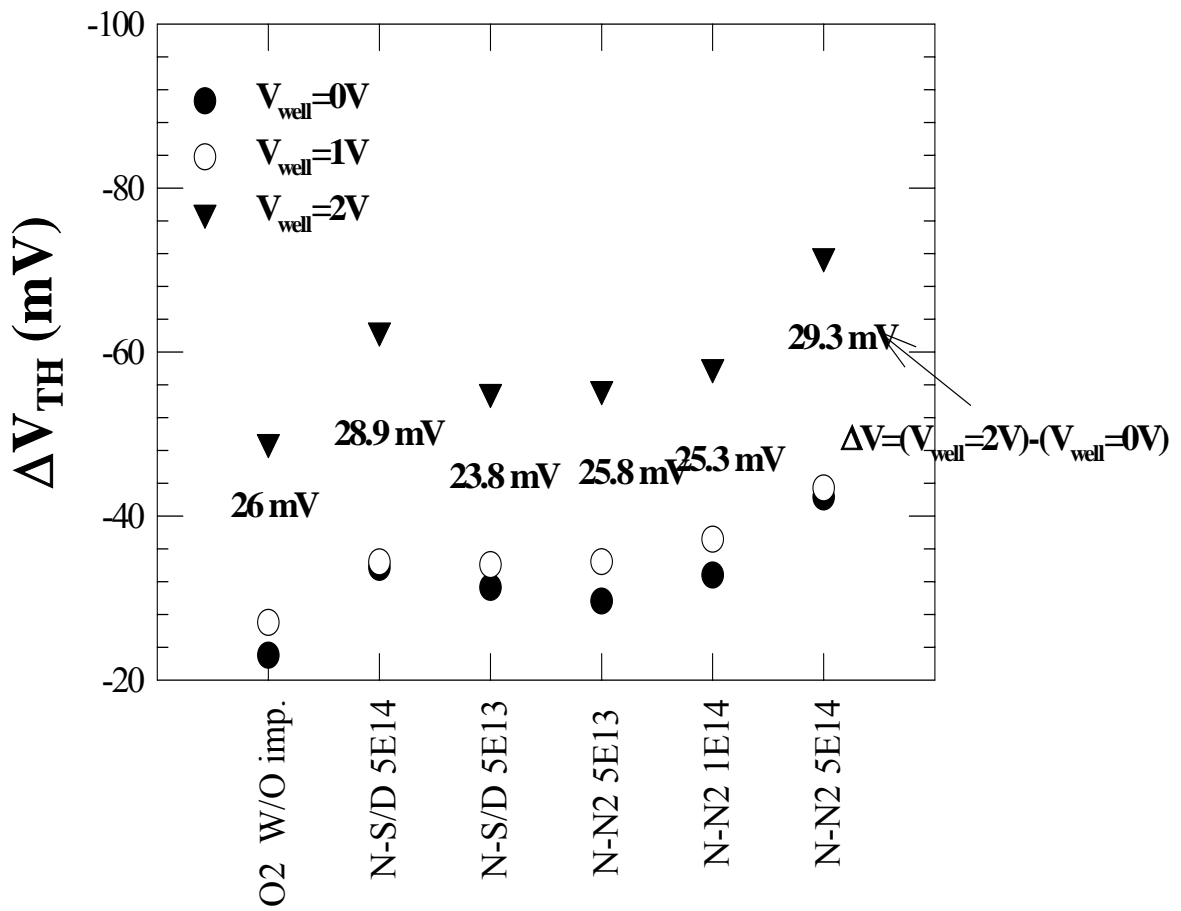
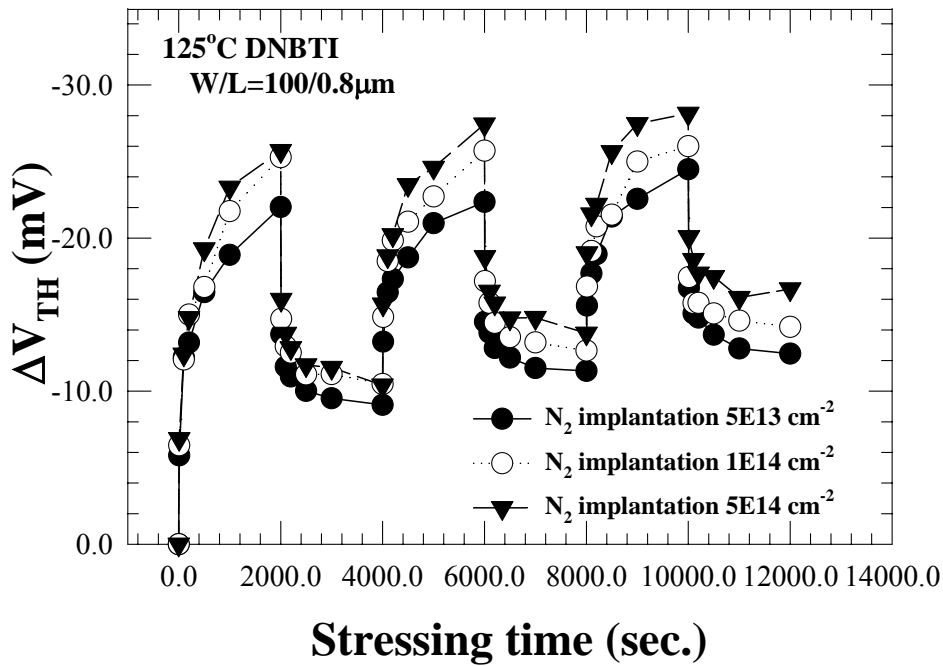
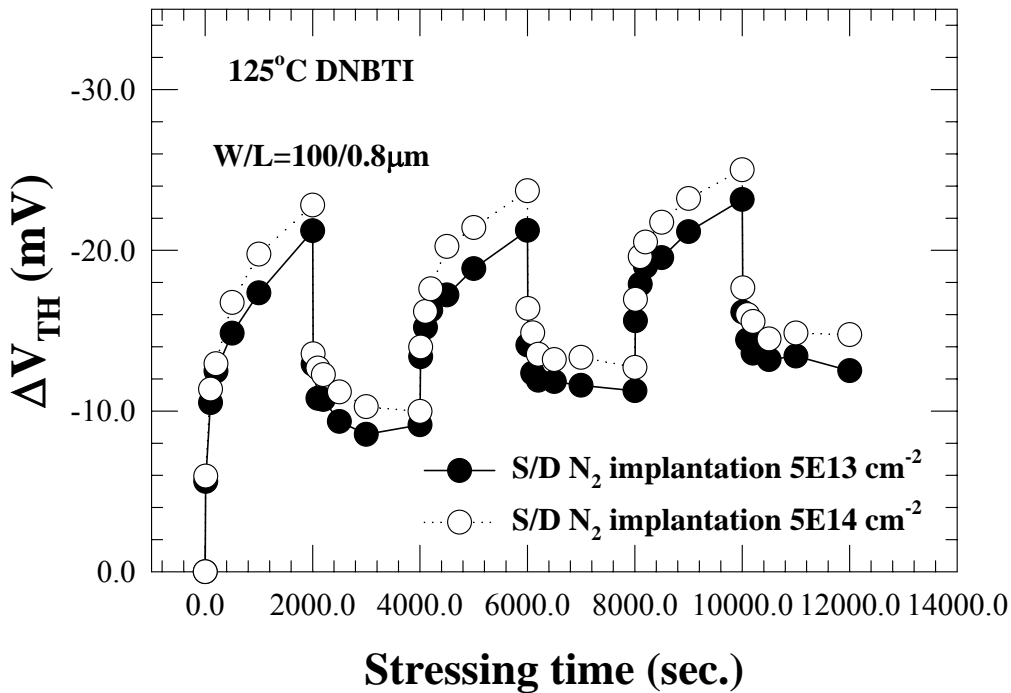


Fig. A.5 The threshold voltage degradation for pMOSFETs with different well biases: $V_{\text{well}}=0, 1, 2$ V, respectively. The stressing condition is 125°C , $E_{\text{OX}}=13$ MV/cm. (N_2O oxide: 10kev, 5×10^{13} , 10^{14} , 5×10^{14} cm^{-2} , and O_2 oxide: w/o implantation.)



(a)



(b)

Fig. A.6 (a) Stress time dependence of threshold voltage degradation for pMOSFETs with different nitrogen implant doses (i.e., 5×10^{13} , 10^{14} , $5 \times 10^{14}\text{ cm}^{-2}$) in (a) the channel (b) and (b) the S/D extension. $E_{OX}=13\text{ MV/cm}$ for “high” state and $V_G=1\text{ V}$ for “low” state. The temperature is kept at $125\text{ }^\circ\text{C}$, and all other terminals (source, drain, well, and substrate) are grounded under both conditions.

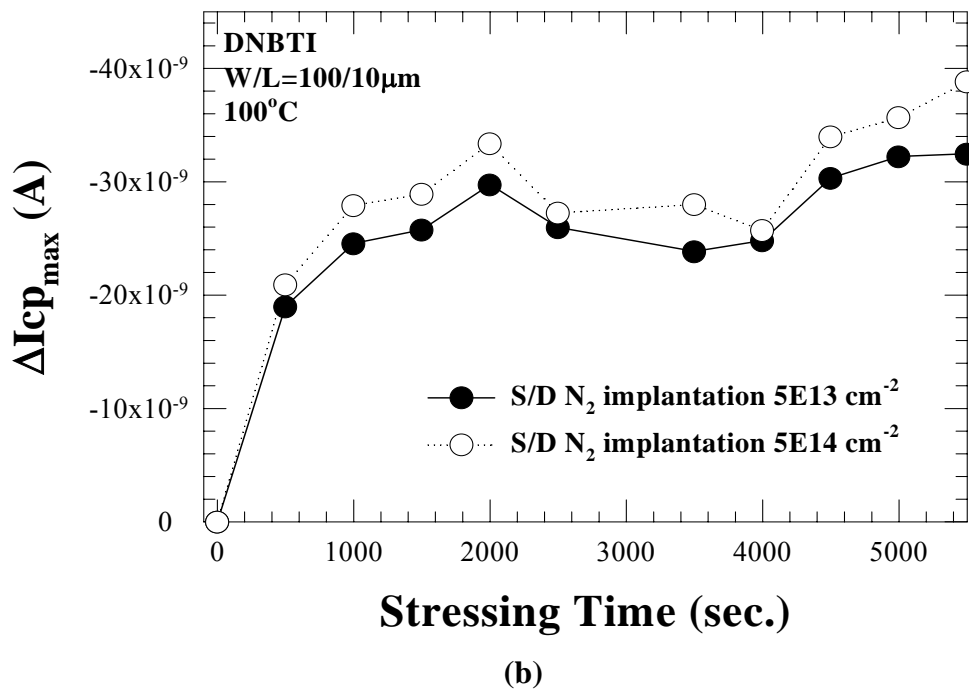
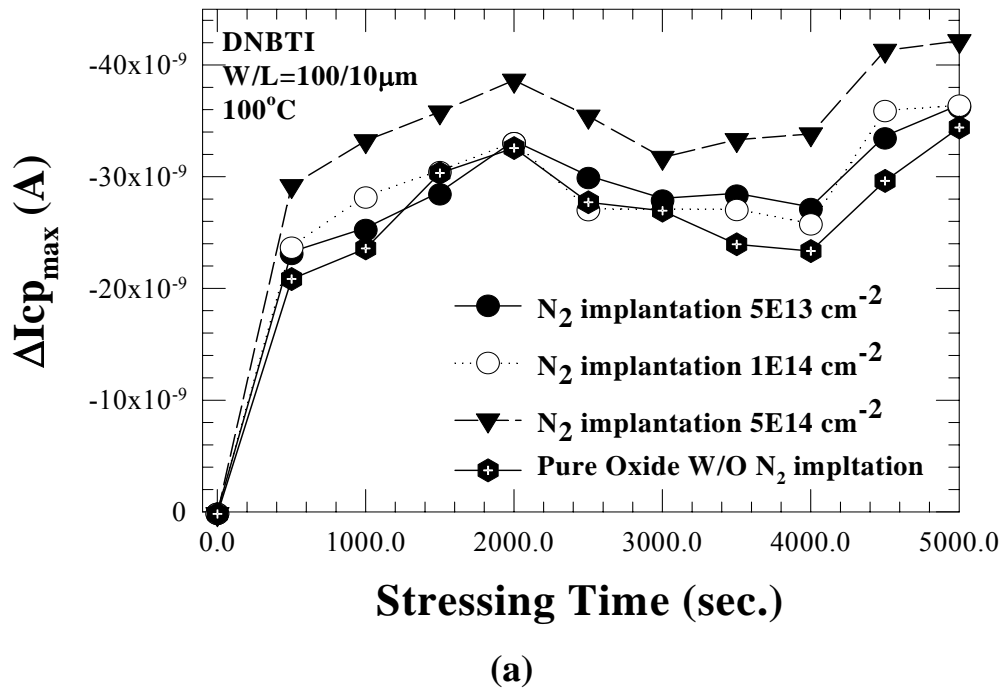


Fig. A.7 Stress time dependence of maximum charging current ($L/W=10/100 \mu\text{m}$) for pMOSFETs with different nitrogen implant doses (N_2O oxide: 5×10^{13} , 10^{14} , $5 \times 10^{14} \text{ cm}^{-2}$, and O_2 oxide: w/o implantation) in (a) the channel and (b) the source/drain extension. $E_{\text{OX}}=13 \text{ MV/cm}$ for the “high” state and $V_{\text{G}}=1 \text{ V}$ for the “low” state. The temperature is kept at $100 \text{ }^\circ\text{C}$, and all other terminals (source, drain, well, and substrate) are grounded under both conditions.

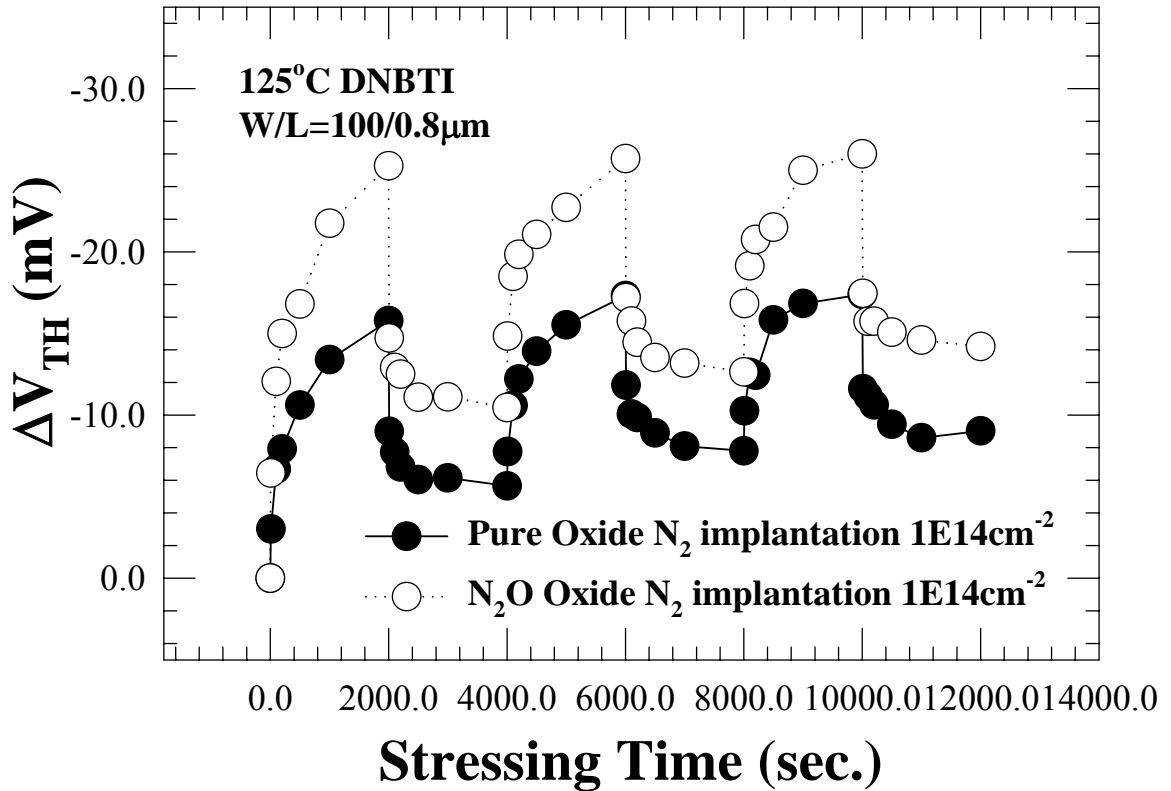
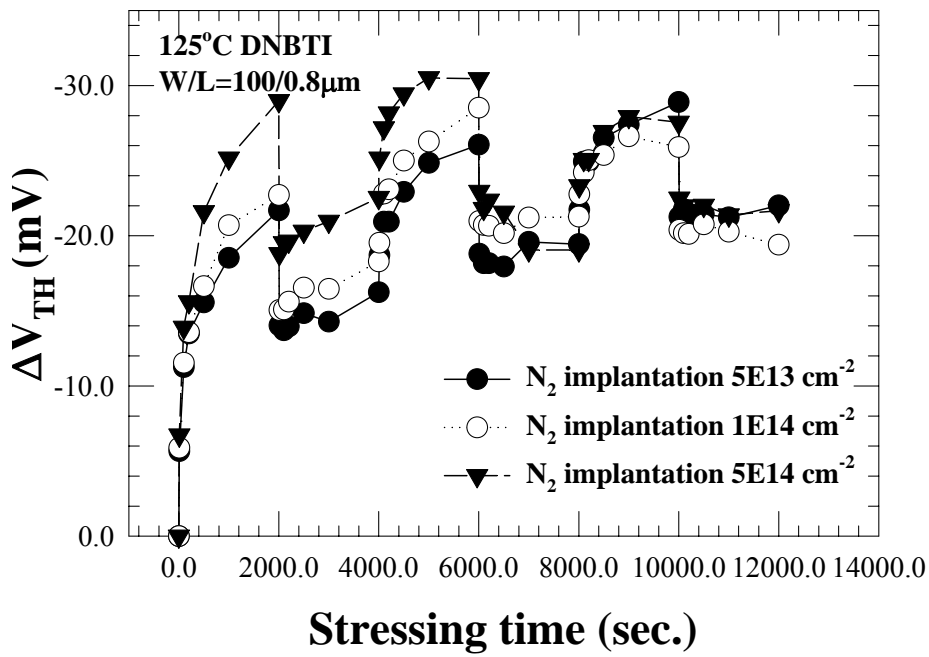
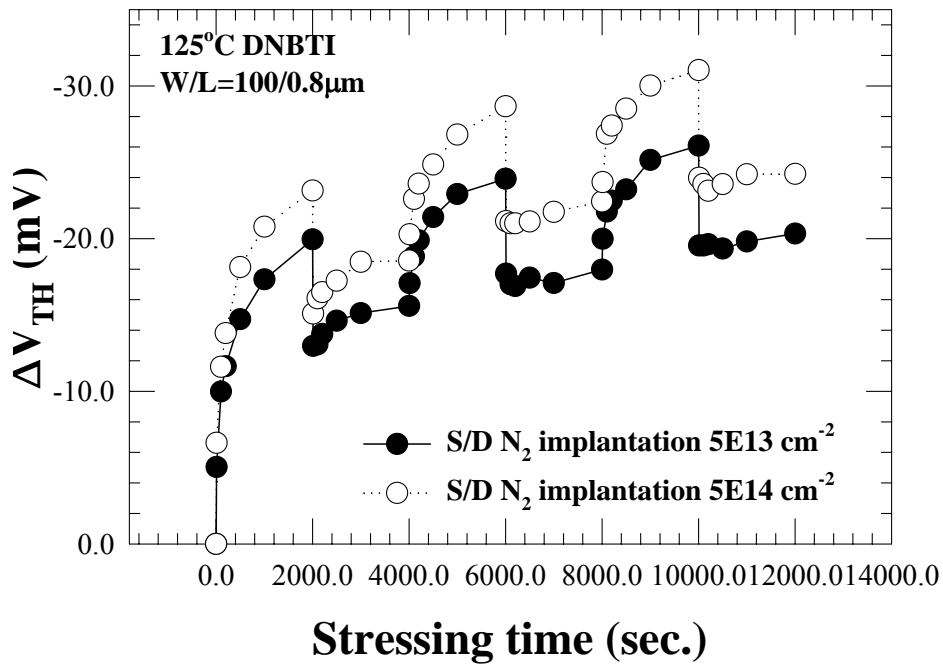


Fig.A.8 Stress time dependence of threshold voltage degradation for pMOSFETs with different nitrogen implant doses (N₂O oxide: 10keV, 5×10¹³ cm⁻², O₂ oxide: 10 keV, 5×10¹³ cm⁻², respectively.) in (a) the channel and (b) the source/drain extension. The conditions of “high” state was for 125 °C, E_{OX}=13 MV/cm for the “high” state and V_G=1 V for the “low” state. The temperature is kept at 125 °C, and all other terminals (source, drain, well, and substrate) are grounded under both conditions.



(a)



(b)

Fig. A.9 Stress time dependence of threshold voltage degradation for N₂O-oxide pMOSFETs with different nitrogen implant doses (5×10^{13} , 10^{14} , 5×10^{14} cm⁻²) in (a) the channel and (b) the S/D extension. The conditions of “high” state ss for 125 °C, $E_{OX}=13$ MV/cm for the “high” state and $E_{OX}=-13$ MV/cm for the “low” state. The temperature is kept at 125 °C, , and all other terminals (source, drain, well, and substrate) are grounded under both conditions.